

# Formulation and Behavior of Epoxy Coating Reinforced with Graphene Oxide-Hollow Mesoporous Silicon Dioxide for Corrosion Protection of Steel Structure

**Nuratirah Rusli**

Department of Mechanical Engineering, Universiti Teknologi PETRONAS, Seri Iskandar, Perak, Malaysia  
nuratirah\_18002432@utp.edu.my

**Mazli Mustapha**

Department of Mechanical Engineering, Universiti Teknologi PETRONAS, Seri Iskandar, Perak, Malaysia  
mazli.mustapha@utp.edu.my (corresponding author)

**Mohd Nurhadi Sahat**

Department of Mechanical Engineering, Universiti Teknologi PETRONAS, UTP, Perak, Malaysia  
mohd\_19000771@utp.edu.my

**Thotiren Jegathesan**

Department of Mechanical Engineering, Universiti Teknologi PETRONAS, Seri Iskandar, Perak, Malaysia  
thotiren\_18003690@utp.edu.my

**Nuur Fahanis Che Lah**

Department of Chemical Engineering, Universiti Teknologi PETRONAS, Seri Iskandar, Perak, Malaysia  
fahanis.chelah@utp.edu.my

**Shahrul Kamaruddin**

Department of Mechanical Engineering, Universiti Teknologi PETRONAS, Seri Iskandar, Perak, Malaysia  
eshahrul.k@utp.edu.my

Received: 7 July 2025 | Revised: 13 August 2025 and 27 August 2025 | Accepted: 2 September 2025

Licensed under a CC-BY 4.0 license | Copyright (c) by the authors | DOI: <https://doi.org/10.48084/etasr.13220>

## ABSTRACT

This study reports the synthesis of graphene oxide-hollow mesoporous silicon dioxide (GO-SiO<sub>2</sub>) hybrid nanostructures and their incorporation into epoxy coatings at loadings of 0.1 wt% and 0.2 wt% using stirring and ultrasonication methods. The functionalization of silicon dioxide (SiO<sub>2</sub>) Nanoparticles (NPs) with 3-(aminopropyl)triethoxysilane (APTES) improved dispersion within the epoxy matrix, overcoming the agglomeration challenge of GO. Fourier Transform Infrared Spectroscopy (FTIR) analysis confirmed the successful formation of the GO-SiO<sub>2</sub> hybrids and validated their role as effective reinforcing agents within the coating system, while the corrosion protection performance and mechanical adhesion strength of the coatings were systematically evaluated using Electrochemical Impedance Spectroscopy (EIS) and pull-off adhesion tests, respectively. The results indicated that GO-SiO<sub>2</sub>/epoxy (GO-SiO<sub>2</sub>/EP) coatings provided superior corrosion resistance and adhesion compared to GO/epoxy (GO-EP) and neat epoxy coatings, with 0.2 wt% GO-SiO<sub>2</sub> prepared by ultrasonication showing the best performance. These

findings highlight the potential of GO-SiO<sub>2</sub>/EP nanocomposite coatings for corrosion protection of steel structures.

**Keywords-**epoxy coating; graphene oxide; mesoporous silicon dioxide; Electrochemical Impedance Spectroscopy (EIS); corrosion

## I. INTRODUCTION

Corrosion remains a leading cause of mechanical failure in metallic structures, resulting in significant material loss and structural degradation. As a preventive corrosion measure, organic polymer coatings are widely used as protective barriers; however, their long-term performance is compromised by mechanical damage, cracking, and permeability to corrosive agents such as water and oxygen. Once coating integrity is compromised, these coatings become less effective, particularly in environments where inspection and maintenance are difficult. Additionally, as reported in [1], grain size plays a critical role in corrosion behavior, and although grain refinement can suppress localized corrosion, general corrosion rates may increase with decreasing grain size, especially under active corrosion conditions.

In practical applications, external corrosion of steel pipelines is predominantly caused by corrosive soils, accounting for up to 67% of reported failures, followed by issues arising from dissimilar metals (12%), coating degradation (10%), and stray electrical currents (4%) [2]. Therefore, to mitigate such failures, corrosion mitigation strategies should address both environmental aggressiveness and intrinsic material vulnerabilities [3].

One of the widely adopted approaches for protecting offshore and buried steel structures is surface functionalization, particularly through the application of organic coatings [4]. However, harsh service conditions in offshore environments, including ultraviolet radiation, temperature fluctuations, and biological fouling, pose significant challenges to conventional coatings, prompting the need for more resilient systems. In parallel with synthetic protection strategies, environmentally friendly corrosion inhibitors such as *Lophatherum gracile* extract have demonstrated promising corrosion inhibition performance by forming adsorbed protective layers on steel surfaces in acidic environments [5]. However, despite their effectiveness under mild conditions, their limited durability in aggressive environments underscores the need for more resilient coating systems.

Accordingly, this study focuses on enhancing epoxy coatings through the incorporation of graphene oxide-silicon dioxide (GO-SiO<sub>2</sub>) nanofillers to achieve long-term corrosion resistance in aggressive service conditions. The first objective was to synthesize GO-SiO<sub>2</sub> hybrids and optimize their dispersion within the epoxy matrix using techniques such as ultrasonication and stirring. The second objective was to assess the corrosion protection performance of the developed coatings using Electrochemical Impedance Spectroscopy (EIS), pull-off adhesion testing, and exposure to CO<sub>2</sub>-rich environments. By analyzing the synergistic interaction between GO-SiO<sub>2</sub> nanofillers and the epoxy matrix, this research seeks to develop a durable nanocomposite coating capable of providing effective

and sustained corrosion protection for steel structures in aggressive service conditions.

## II. METHODOLOGY

### A. Formulation of High-Quality GO-SiO<sub>2</sub> Hybrid

The procedure for formulating high-quality GO-SiO<sub>2</sub> hybrids begins with the preparation of the raw materials, graphene oxide (GO) and silicon dioxide (SiO<sub>2</sub>). This process involves i) functionalizing SiO<sub>2</sub> Nanoparticles (NPs) with 3-(aminopropyl) triethoxysilane (APTES) to produce amino-terminated SiO<sub>2</sub> particles, and ii) mixing the APTES-functionalized SiO<sub>2</sub> with GO to produce the GO-SiO<sub>2</sub> hybrids, which is essential to prevent the agglomeration of the GO-SiO<sub>2</sub> hybrid within the epoxy matrix.

For the functionalization process, 50 g of toluene and 0.5 grams of SiO<sub>2</sub> powder were mixed and stirred at room temperature. Subsequently, 0.5 g of APTES was added to the suspension, and stirring continued until a yellow translucent dispersion was obtained. Then, the reaction mixture was refluxed for an additional 24 h. After refluxing, the solvent was removed using a rotary evaporator until a dry residue was obtained. The resulting f-SiO<sub>2</sub> powder was further dried overnight at 50 °C to eliminate residual solvent.

Surface decoration of GO was performed by dispersing it in N,N-Dimethylformamide (DMF), which served as the medium for the attachment process. Since GO was supplied in powder form, a solvent selection methodology was employed to achieve a fine dispersion in DMF. Specifically, 0.08 g of GO powder was dispersed in 50 mL of DMF, followed by ultrasonication and heating to 70 °C. Subsequently, the prepared Functionalized silicon dioxide (f-SiO<sub>2</sub>) powder was added to the GO suspension and ultrasonicated to promote uniform mixing. The mixture was then stirred for 5 h under continuous heating at 105 °C to facilitate condensation reactions between silanol groups and GO functional groups, leading to strong interfacial bonding between APTES-modified SiO<sub>2</sub> and GO, consistent with previous reports [6]. After completion of the reaction, the mixture was allowed to cool to room temperature, and the GO-SiO<sub>2</sub> hybrids were collected and dried in a vacuum oven at 40 °C for at least 3 h.

The procedure was conducted with a mixing ratio of 1:5 for GO to f-SiO<sub>2</sub> to achieve a thin-layered hybrid structure, which is favorable for achieving uniform dispersion within polymer matrices compared to multilayered configurations.

### B. Formulation of Highly Dispersed GO-SiO<sub>2</sub> Hybrid in Epoxy through Ultrasonication and Stirring Method

The successful attachment of SiO<sub>2</sub> NPs onto the GO surface results in GO-SiO<sub>2</sub> hybrids that likely possess an exfoliated structure. However, their effective dispersion within the epoxy matrix depends strongly on the incorporation method. To evaluate and optimize filler dispersion, two distinct mixing

strategies were employed: ultrasonication (U) and mechanical stirring (S). Ultrasonication is a widely used method for dispersing fillers into polymers, employing high-frequency sound waves to create tiny bubbles that collapse, generating shockwaves to break larger particles into smaller ones and disperse GO-SiO<sub>2</sub> evenly throughout the epoxy coating. However, ultrasonication may introduce drawbacks such as residual solvent retention and potential structural damage to fillers. Therefore, mechanical stirring was also investigated as an alternative method to assess whether the combined presence of GO and SiO<sub>2</sub> could synergistically reduce agglomeration without excessive energy input. The stirring approach was hypothesized to allow GO sheets to behave as independent entities, thereby mitigating re-agglomeration while maintaining effective filler dispersion.

The preparation of highly dispersed GO-SiO<sub>2</sub> hybrids in epoxy involved three types of coatings: bare epoxy, GO/epoxy (GO/EP), and GO-SiO<sub>2</sub>/epoxy (GO-SiO<sub>2</sub>/EP). A total of nine coating formulations with varying filler contents and dispersion techniques were prepared, as summarized in Table I. All coatings were applied onto degreased and sandblasted steel substrates using a paintbrush, ensuring a uniform dry film thickness of 250 ± 5 μm. Details about the composition of each mixture are presented in Table II. Before performance evaluation, all three types of coatings were cured at room temperature for one week before performance evaluation.

TABLE I. COATING PREPARATION MATRIX

Sample no.	Coating Type
A	Bare Epoxy 0wt%
B	GO-SiO <sub>2</sub> /EP (U) 0.1wt%
C	GO-SiO <sub>2</sub> /EP (U) 0.2wt%
D	GO-SiO <sub>2</sub> /EP (S) 0.1wt%
E	GO-SiO <sub>2</sub> /EP (S) 0.2wt%
F	GO/EP (U) 0.1wt%
G	GO/EP (U) 0.2wt%
H	GO/EP (S) 0.1wt%
I	GO/EP (S) 0.2wt%
Total	9 samples

TABLE II. SUMMARY OF THE AMOUNT OF EPOXY AND HARDENER USED FOR ULTRASONICATION, STIRRING, AND BARE EPOXY SAMPLES

Bare Epoxy	0 wt%	
Epoxy: Hardener	2:1	
Amount in Mixture	28g of epoxy with 14g of hardener	
GO-SiO <sub>2</sub> /EP (S)	0.1 wt%	0.2 wt%
GO/EP (S)		
GO-SiO <sub>2</sub> /EP (U)		
GO/EP (U)		
Epoxy: Hardener	2:1	
Amount in Mixture	0.028 g of GO-SiO <sub>2</sub> and GO powder with 28 g of epoxy and 14 g of hardener	0.056 g of GO-SiO <sub>2</sub> and GO powder with 28 g of epoxy and 14 g of hardener

### C. Strategy 1: Ultrasonication Technique

For the ultrasonication-based preparation, GO-SiO<sub>2</sub> powder was first dispersed in 5 mL of acetone and ultrasonicated for 1 h. The dispersion was then added to a predetermined quantity

of polyamide hardener and subjected to further ultrasonication for 30 min. Once a uniform dispersion within the hardener was achieved, the mixture was heated to 70 °C and stirred continuously for 3 h to evaporate residual solvent. The mixture was subsequently vacuum-heated for an additional hour to ensure complete degassing and solvent removal. Afterwards, the hardener mixture was combined with the stoichiometric amount of epoxy resin at room temperature, and the mixture was stirred for 15 min using a magnetic stirrer to ensure homogeneity.

### D. Strategy 2: Stirring Technique

For the stirring-based preparation, GO-SiO<sub>2</sub> hybrids were mixed with a predetermined amount of polyamide hardener using magnetic stirring at a constant speed of 1400 rpm for 1 h. The mixture was then degassed in a vacuum oven for an additional hour to remove entrapped air. Epoxy resin was subsequently added at a stoichiometric ratio of 2:1 (epoxy:hardener), and the mixture was stirred to achieve uniform dispersion. The same procedure was followed for preparing GO/EP coatings.

## III. RESULTS AND DISCUSSION

### A. FTIR Analysis of APTES, SiO<sub>2</sub>, f-SiO<sub>2</sub>, GO, and GO-SiO<sub>2</sub> Hybrids

Fourier Transform Infrared Spectroscopy (FTIR) spectroscopy provides a powerful analytical tool for identifying functional groups and chemical interactions, offering spectra that can be compared against standard libraries with reference spectra [7, 8]. It has been applied in various studies, such as the analysis of oxygen functionalities in thermally reduced GO and NP adsorption at solid-liquid interfaces [6, 9-11].

In this case, FTIR analysis was employed to verify the successful functionalization of SiO<sub>2</sub> NPs with APTES. Figure 1 presents the FTIR spectra of pure APTES, unmodified SiO<sub>2</sub>, and APTES-functionalized SiO<sub>2</sub> (f-SiO<sub>2</sub>).

The FTIR spectrum of pure APTES exhibits characteristic absorption bands consistent with its molecular structure. Specifically, the broad absorption band at 3,368.71 cm<sup>-1</sup> is attributed to N-H stretching vibrations of the primary amine group (-NH<sub>2</sub>). In addition, peaks observed at 2,974.90, 2,927.91, and 2,887.31 cm<sup>-1</sup> correspond to C-H stretching from the alkyl chains. Additional peaks at 1,079.40 cm<sup>-1</sup> (aliphatic CH<sub>2</sub>/CH<sub>3</sub>), 957.12 cm<sup>-1</sup> (C-O stretching), and 790.96 cm<sup>-1</sup> (Si-O stretching) further validate the presence of APTES functional groups [12-15].

The FTIR spectrum of unmodified SiO<sub>2</sub> shows dominant signals at 1,084.17 cm<sup>-1</sup>, corresponding to Si-O-Si stretching, and peaks at 806.65 and 463.27 cm<sup>-1</sup> from bending vibrations in the siloxane network. A minor peak at 3,457.01 cm<sup>-1</sup> indicates O-H stretching due to surface hydroxyl groups or adsorbed water [15].

Furthermore, the FTIR spectrum of f-SiO<sub>2</sub> exhibits both preserved silica-related peaks and new absorption bands originating from APTES. The primary Si-O-Si peak at 1,083.71 cm<sup>-1</sup> remains prominent, confirming the structural integrity of the silica framework. New peaks at 2,934.83 cm<sup>-1</sup> reflect C-H

stretching from the propyl groups of APTES, while peaks in the 1,635.04 to 1,562.44  $\text{cm}^{-1}$  range correspond to N-H bending vibrations, indicating the presence of amine groups from APTES. A reduced O-H peak at 3,434.48  $\text{cm}^{-1}$  suggests that surface hydroxyl groups were consumed during silanization, forming covalent Si-O-Si bonds with APTES [16].

Additionally, Figure 2 presents the FTIR spectra of f-SiO<sub>2</sub>, GO, and the resulting GO-SiO<sub>2</sub> hybrid. The f-SiO<sub>2</sub> spectrum in Figure 2 is intentionally reproduced from Figure 1 to enable direct comparison with GO and GO-SiO<sub>2</sub> and to highlight spectral changes arising from hybrid formation.

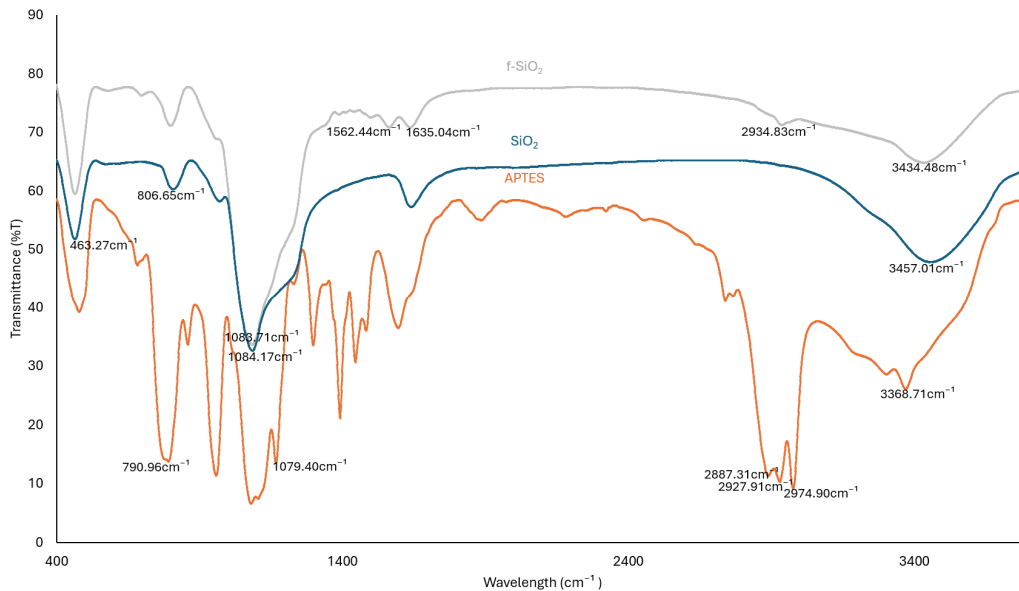


Fig. 1. FTIR spectra of APTES, SiO<sub>2</sub> NPs, and APTES-functionalized SiO<sub>2</sub> NPs.

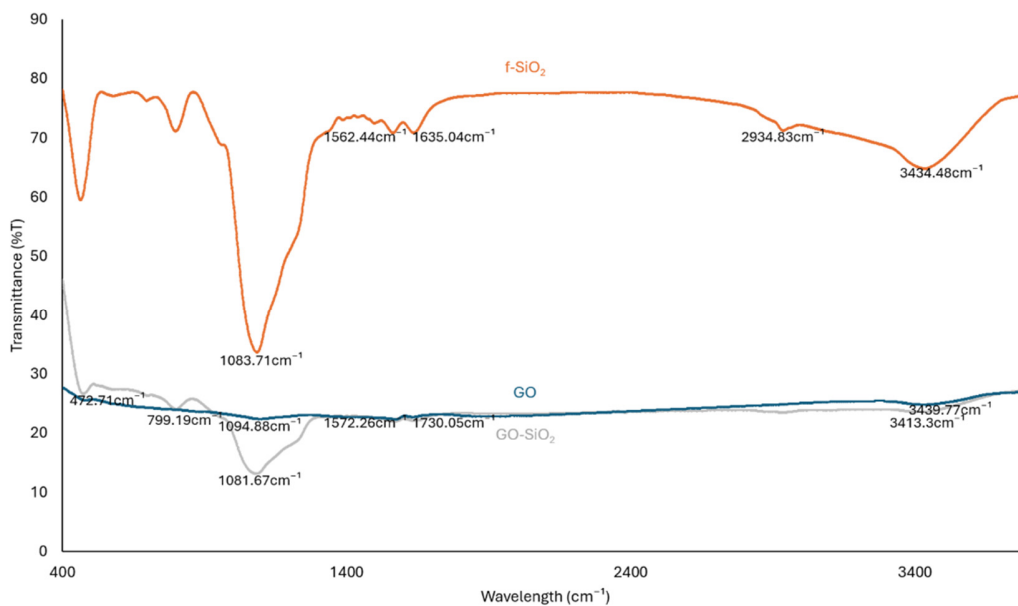


Fig. 2. FTIR spectra for APTES-functionalized SiO<sub>2</sub>, GO, and GO-SiO<sub>2</sub>.

GO exhibits a distinct spectral fingerprint due to its various oxygen-containing functional groups. Firstly, the broad O-H stretching band at 3,439.77  $\text{cm}^{-1}$  indicates hydroxyl functionalities on GO's surface. In addition, the sharp peak at 1,730.05  $\text{cm}^{-1}$  confirms the presence of carbonyl (C=O) groups, primarily from carboxylic acids, while the signal at 1,094.88

$\text{cm}^{-1}$  arises from overlapping epoxy, alkoxy, and phenolic C-O stretching vibrations. The peak at 1,572.26  $\text{cm}^{-1}$  corresponds to C=C stretching in aromatic regions of unoxidized graphene domains, providing insights into the degree of oxidation and remaining graphitic structure [8].

Moreover, the FTIR spectrum of the GO-SiO<sub>2</sub> hybrid demonstrates clear evidence of chemical interaction between GO and f-SiO<sub>2</sub>. Specifically, key absorption bands at 1,566.47 cm<sup>-1</sup>, 1,081.67 cm<sup>-1</sup>, and 799.19 cm<sup>-1</sup> are attributed to N-H, Si-O-C, and Si-O-Si linkages, respectively, confirming successful integration of the two components. Notably, the disappearance of the GO carbonyl peak at 1,730.05 cm<sup>-1</sup> suggests that carboxyl groups on GO participate in chemical bonding with amine-functionalized silica. Additionally, the reduced intensity of the epoxide-related band around 1,080 cm<sup>-1</sup> indicates partial consumption of epoxy groups during the functionalization process. The reduced intensity and narrowing of the O-H stretching band in the GO-SiO<sub>2</sub> hybrid compared to GO further suggest involvement of hydroxyl groups in interfacial bonding. Lastly, the low-frequency band at 472.71 cm<sup>-1</sup> corresponds to Si-O bending vibrations, confirming the presence of the silica framework within the hybrid structure. Collectively, these spectral changes provide strong evidence of chemical interaction between GO and f-SiO<sub>2</sub>, supporting the formation of a well-integrated hybrid filler suitable for epoxy-based corrosion-protection coatings [11].

### B. EIS Analysis

EIS was carried out at Open Circuit Potential (OCP), with data recorded every seven days to evaluate the composite coating's protective properties. The EIS experiments were performed in a CO<sub>2</sub>-saturated saltwater environment to replicate conditions similar to the interiors of multiphase pipelines. In such environments, CO<sub>2</sub> reacts with water to form carbonic acid, which accelerates corrosion of carbon steel [17]. EIS measurements were performed over a frequency range of 10<sup>4</sup> Hz to 10<sup>-2</sup> Hz to capture both high- and low-frequency electrochemical responses. Bode magnitude plots were used to evaluate impedance values across frequencies, offering insight into corrosion kinetics and coating integrity [18-22]. For instance, a bigger magnitude at specific frequencies suggests better corrosion protection, whereas lower values might indicate the start of corrosion processes [21]. Additionally, Bode plots are especially helpful when evaluating the performance of nanocomposites [23].

The magnitude Bode plots for the nine samples are presented in Figures 4 and 5 based on GO-SiO<sub>2</sub> wt% percentage used. Both plots reveal that bare epoxy exhibits the lowest impedance, with a value of 1.97×10<sup>8</sup> Ω at the lowest measured frequency, indicating limited corrosion protection. In contrast, composites containing fillers have a much greater impedance, suggesting improved corrosion resistance. Both GO and GO-SiO<sub>2</sub> composite coatings greatly improved impedance, while GO-SiO<sub>2</sub> outperformed GO in every case. This shows that functionalizing GO with SiO<sub>2</sub> improves its dispersion and interaction within the epoxy matrix, resulting in higher corrosion resistance, which is also supported in [24]. Furthermore, the method of filler incorporation played a critical role. For both filler types, samples made with ultrasonication consistently had a greater impedance than those prepared with magnetic stirring. This suggests that ultrasonication promoted a more uniform dispersion of fillers in the epoxy, hence increasing the coating's barrier qualities [6].

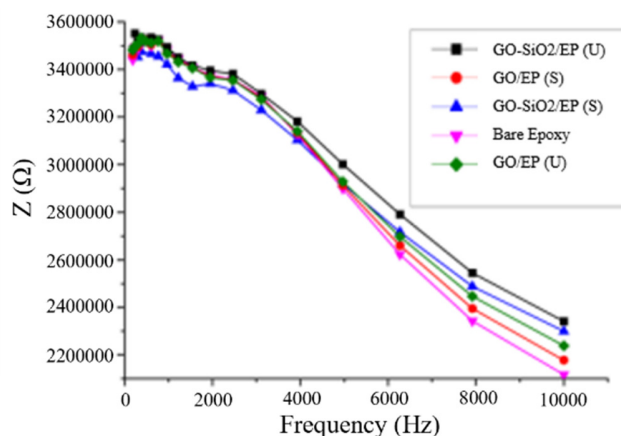


Fig. 3. Magnitude Bode Plot (0.1wt%).

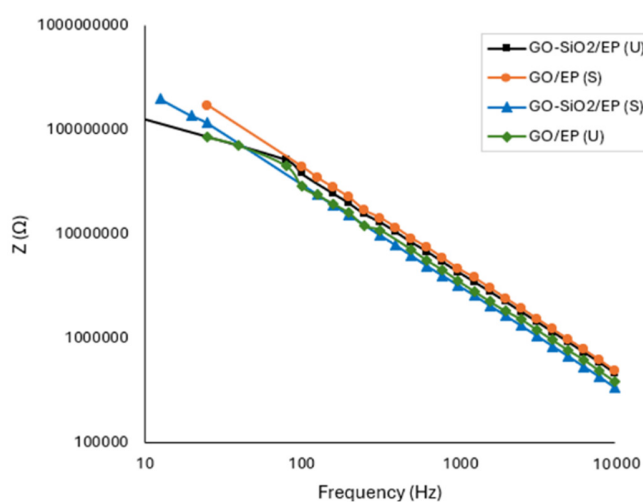


Fig. 4. Magnitude Bode Plot (0.2wt%).

Additionally, increasing the GO-SiO<sub>2</sub> concentration from 0.1 wt% to 0.2 wt% further enhanced corrosion protection. The 0.2 wt% GO-SiO<sub>2</sub>/EP sample prepared via ultrasonication exhibited the highest impedance (1.40×10<sup>8</sup> Ω at the lowest frequency), significantly surpassing GO/EP (U) at the same concentration (8.51×10<sup>7</sup> Ω). The 0.2 wt% concentration is likely the ideal quantity of filler for forming an effective barrier, while ultrasonication assures uniform dispersion. A higher concentration of GO-SiO<sub>2</sub> minimizes the likelihood of micro-defects in the coating, which might allow corrosive agents to penetrate it [25].

### C. Comparison with Literature

To highlight the novelty and performance of our GO-hollow mesoporous SiO<sub>2</sub> hybrid, we compared it with recent works on SiO<sub>2</sub>/GO epoxy composites, silica sol-gel coatings, and other GO-inorganic hybrids. Across these studies, our formulation achieved higher low-frequency impedance and superior barrier longevity, confirming the effectiveness of our functionalization and dispersion approach [26-29]. These comparisons are summarized in Table III.

TABLE III. COMPARISONS OF THE KEY FINDINGS IN THIS STUDY AGAINST PREVIOUSLY PUBLISHED WORKS

Study & Years	Filler System	Test Media	Key Findings	Comparison with This Study
[26]	SiO <sub>2</sub> /GO in epoxy	Marine saline solution	Improved EIS	Higher low-freq. impedance, longer durability
[27]	Silica sol-gel coatings on steel	Aqueous media	Performance depends on synthesis	More stable response without sol-gel limits
[28]	SiO <sub>2</sub> -GO in PU acrylic	Neutral saline	Transmission Electron Microscopy (TEM) evidence, better resistance	Higher impedance & adhesion under CO <sub>2</sub> -saline
[29]	GO-ZSM-5-epoxy	3.5 wt% NaCl	Strong Impedance Parameter (IP) increase vs. neat epoxy	Comparable or higher impedance with simpler filler

#### D. Pull-Adhesion Test

Pull-off adhesion tests were conducted on all nine coating formulations to quantify the force (coating-substrate interfacial strength) required to detach the coating from the steel substrate [25]. Two dollies were attached per sample, ensuring consistency with the coating thickness. Results, presented in Figure 6, indicate that GO-SiO<sub>2</sub>/EP (U) at 0.2 wt% exhibited the highest adhesion strength, demonstrating the synergistic effect of functionalization and ultrasonication.

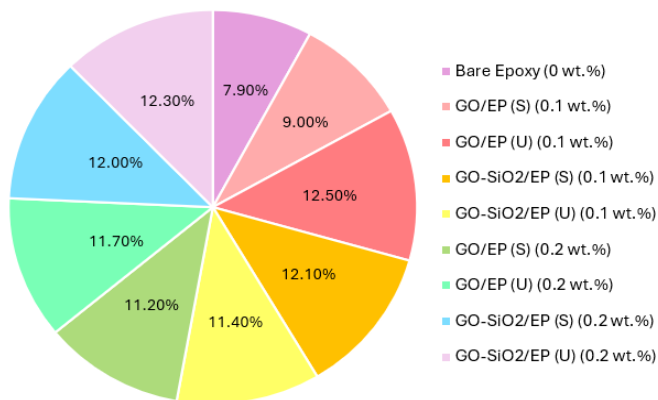


Fig. 5. Total % of pull-adhesion strength for each sample.

Other formulations, such as GO/EP (U) 0.1 wt% and GO-SiO<sub>2</sub>/EP (S) 0.2 wt%, also displayed improved adhesion compared to bare epoxy, highlighting the positive contribution of nanofillers to interfacial bonding. Bare epoxy showed the lowest adhesion (7.9%), confirming that unmodified epoxy coatings have limited substrate interaction. Moreover, samples treated with ultrasonication had a somewhat larger contribution than those generated by stirring, indicating that ultrasonication increases dispersion and adhesion strength. This implies that

nanofiller addition and processing methods have a considerable impact on epoxy adhesion performance [30].

#### IV. CONCLUSION

This study successfully developed graphene oxide-hollow mesoporous silicon dioxide (GO-SiO<sub>2</sub>) hybrid fillers and integrated them into epoxy coatings at loadings of 0.1 wt% and 0.2 wt% using both mechanical stirring and ultrasonication dispersion techniques. Functionalization of SiO<sub>2</sub> Nanoparticles (NPs) with 3-(aminopropyl)triethoxysilane (APTES) significantly improved their compatibility with GO and dispersion within the epoxy matrix, mitigating GO agglomeration issues.

Fourier Transform Infrared Spectroscopy (FTIR) analysis confirmed the chemical interactions between GO, SiO<sub>2</sub>, and APTES-functionalized SiO<sub>2</sub>, supporting their role as effective reinforcing agents. Additionally, performance evaluation using Electrochemical Impedance Spectroscopy (EIS) and pull-off adhesion tests revealed that GO-SiO<sub>2</sub>/epoxy (GO-SiO<sub>2</sub>/EP) coatings enhanced both corrosion resistance and interfacial adhesion compared to GO/EP and unmodified epoxy systems. Among the formulations, the 0.2 wt% GO-SiO<sub>2</sub>/EP coating prepared via ultrasonication exhibited the highest impedance values, indicating superior corrosion protection. Nevertheless, both filler concentrations contributed to improved barrier and mechanical properties, demonstrating the effectiveness of GO-SiO<sub>2</sub> nanohybrids in epoxy-based corrosion protection systems for steel substrates.

Future work should focus on optimizing filler synthesis by exploring alternative dispersion strategies, such as high-shear mixing or solvent-assisted techniques. Additional investigation into hybrid nanofillers and multifunctional coating systems may further enhance performance. Lastly, extended electrochemical testing under diverse environmental conditions and real-world exposure scenarios would provide a more comprehensive understanding of long-term coating durability and potential applications across broader structural and industrial contexts.

#### ACKNOWLEDGMENT

The authors gratefully acknowledge the financial support provided by Yayasan Universiti Teknologi PETRONAS through the YUTP-FRG with the cost center of 015LC0- 474.

#### REFERENCES

- [1] H. Miyamoto, "Corrosion of Ultrafine Grained Materials by Severe Plastic Deformation, an Overview," *Materials Transactions*, vol. 57, no. 5, pp. 559–572, 2016, <https://doi.org/10.2320/matertrans.M2015452>.
- [2] H. M. H. Farh, M. E. A. Ben Seghier, and T. Zayed, "A comprehensive review of corrosion protection and control techniques for metallic pipelines," *Engineering Failure Analysis*, vol. 143, Jan. 2023, Art. no. 106885, <https://doi.org/10.1016/j.engfailanal.2022.106885>.
- [3] S. Kumari, A. Saini, and V. Dhayal, "Metal oxide based epoxy coatings for corrosion protection of steel," *Materials Today: Proceedings*, vol. 43, pp. 3105–3109, 2021, <https://doi.org/10.1016/j.matpr.2021.01.587>.
- [4] A. A. Olajire, "Recent advances on organic coating system technologies for corrosion protection of offshore metallic structures," *Journal of Molecular Liquids*, vol. 269, pp. 572–606, Nov. 2018, <https://doi.org/10.1016/j.molliq.2018.08.053>.

- [5] M. I. Haris, Agung, M. Anjas, G. J. B. Houston, N. Qadry, and Fakhruddin, "Development of a Green Corrosion Inhibitor from Lophatherum Gracile Extract for Steel Protection," *Engineering, Technology & Applied Science Research*, vol. 15, no. 1, pp. 19253–19260, Feb. 2025, <https://doi.org/10.48084/etasr.8609>.
- [6] B. Gou, X. Song, Z. Wu, and X. Chen, "Effects of Silicon Dioxide/Graphene Oxide Hybrid Modification on Curing Kinetics of Epoxy Resin," *ACS Omega*, vol. 7, no. 41, pp. 36551–36560, Oct. 2022, <https://doi.org/10.1021/acsomega.2c04505>.
- [7] Q. Zhu, R. Zhou, J. Liu, J. Sun, and Q. Wang, "Recent Progress on the Characterization of Cellulose Nanomaterials by Nanoscale Infrared Spectroscopy," *Nanomaterials*, vol. 11, no. 5, May 2021, Art. no. 1353, <https://doi.org/10.3390/nano11051353>.
- [8] V. Brusko, A. Khannanov, A. Rakhmatullin, and A. M. Dimiev, "Unraveling the infrared spectrum of graphene oxide," *Carbon*, vol. 229, Oct. 2024, Art. no. 119507, <https://doi.org/10.1016/j.carbon.2024.119507>.
- [9] M. Acik *et al.*, "The Role of Oxygen during Thermal Reduction of Graphene Oxide Studied by Infrared Absorption Spectroscopy," *The Journal of Physical Chemistry C*, vol. 115, no. 40, pp. 19761–19781, Oct. 2011, <https://doi.org/10.1021/jp2052618>.
- [10] I. A. Mudunkotuwa, A. A. Minshid, and V. H. Grassian, "ATR-FTIR spectroscopy as a tool to probe surface adsorption on nanoparticles at the liquid–solid interface in environmentally and biologically relevant media," *The Analyst*, vol. 139, no. 5, pp. 870–881, 2014, <https://doi.org/10.1039/C3AN01684F>.
- [11] D.-H. Tsai, M. Davila-Morris, F. W. DelRio, S. Guha, M. R. Zachariah, and V. A. Hackley, "Quantitative Determination of Competitive Molecular Adsorption on Gold Nanoparticles Using Attenuated Total Reflectance–Fourier Transform Infrared Spectroscopy," *Langmuir*, vol. 27, no. 15, pp. 9302–9313, Aug. 2011, <https://doi.org/10.1021/la2005425>.
- [12] J. Liu, X. Hao, and X. Zhang, "Structure and Property of Pesticide Intercalation into Laponite Assisted by Silane Coupling Agent," *ChemistrySelect*, vol. 6, no. 33, pp. 8689–8695, Sept. 2021, <https://doi.org/10.1002/slct.202102168>.
- [13] V. Mirzaie *et al.*, "Nano-Graphene Oxide-supported APTES-Spermine, as Gene Delivery System, for Transfection of pEGFP-p53 into Breast Cancer Cell Lines," *Drug Design, Development and Therapy*, vol. 14, pp. 3087–3097, July 2020, <https://doi.org/10.2147/DDDT.S251005>.
- [14] Y. S. Kim and G. S. An, "Optimizing Amine Functionalization of Maghemite Nanoparticles Through Controlled Hydroxylation and Silica Interlayer Engineering," *Processes*, vol. 13, no. 5, May 2025, Art. no. 1575, <https://doi.org/10.3390/pr13051575>.
- [15] J. J. Gutiérrez Moreno, K. Pan, Y. Wang, and W. Li, "Computational Study of APTES Surface Functionalization of Diatom-like Amorphous SiO<sub>2</sub> Surfaces for Heavy Metal Adsorption," *Langmuir*, vol. 36, no. 20, pp. 5680–5689, May 2020, <https://doi.org/10.1021/acs.langmuir.9b03755>.
- [16] E. J. Cueto-Díaz *et al.*, "APTES-Based Silica Nanoparticles as a Potential Modifier for the Selective Sequestration of CO<sub>2</sub> Gas Molecules," *Nanomaterials*, vol. 11, no. 11, Oct. 2021, Art. no. 2893, <https://doi.org/10.3390/nano11112893>.
- [17] A. E.-L. Hany Mohamed, A. Vagif Maharram, A. Leylufur Imran, and I. Teyyub Allahverdi, "Corrosion Protection of Steel Pipelines Against CO<sub>2</sub> Corrosion-A Review," *Chemistry Journal (2012)*, vol. 2, no. 02, pp. 52–63.
- [18] M. Alhamad, V. A. Ricardo Barao, C. Sukotjo, A. Yerokhin, and M. T. Mathew, "Unpredictable Electrochemical Processes in Ti Dental Implants: The Role of Ti Ions and Inflammatory Products," *ACS Applied Bio Materials*, vol. 6, no. 9, pp. 3661–3673, Sept. 2023, <https://doi.org/10.1021/acsbm.3c00235>.
- [19] L. M. B. Lucatero, D. T. Ortega, T. Pandiyan, N. Singh, H. Singh, and T. P. S. Sarao, "Corrosion inhibition studies of cigarette waste on the iron surface in acid medium: electrochemical and surface morphology analysis," *Anti-Corrosion Methods and Materials*, vol. 63, no. 4, pp. 245–255, June 2016, <https://doi.org/10.1108/ACMM-05-2014-1384>.
- [20] C. Mani, R. Karthikeyan, and S. Kannan, "Electrochemical Impedance Analysis on Cryogenically Treated Dissimilar Metal Welding of 316L Stainless Steel and Monel 400 Alloy Using GTAW," *Metals*, vol. 9, no. 10, Oct. 2019, Art. no. 1088, <https://doi.org/10.3390/met9101088>.
- [21] C. Syu, Y. Lin, Y. Yeh, and T. Don, "Preparation of transparent nanocomposites from UV- and thermo-curable epoxyacrylate and graphene oxide for the application of corrosion protection coatings," *Polymer International*, vol. 68, no. 10, pp. 1804–1816, Oct. 2019, <https://doi.org/10.1002/pi.5891>.
- [22] M. Saedikhani, S. L. Wijesinghe, and D. J. Blackwood, "Barrier and Sacrificial Protection Mechanisms of Zinc Rich Primers," *Engineering Journal*, vol. 23, no. 4, pp. 223–233, Aug. 2019, <https://doi.org/10.4186/ej.2019.23.4.223>.
- [23] M. Mobin and F. Ansar, "Polythiophene (PTh)–TiO<sub>2</sub>–Reduced Graphene Oxide (rGO) Nanocomposite Coating: Synthesis, Characterization, and Corrosion Protection Performance on Low-Carbon Steel in 3.5 wt % NaCl Solution," *ACS Omega*, vol. 7, no. 50, pp. 46717–46730, Dec. 2022, <https://doi.org/10.1021/acsomega.2c05678>.
- [24] C. Feng, L. Zhu, K. Cao, Z. Yu, and Y. Song, "Difunctional Silicon Dioxide Combined with Graphene Oxide Nanocomposite to Enhance the Anticorrosion Performance of Epoxy Coatings," *ACS Omega*, vol. 7, no. 28, pp. 24134–24144, July 2022, <https://doi.org/10.1021/acsomega.2c00494>.
- [25] S. Pourhashem, M. R. Vaezi, and A. Rashidi, "Investigating the effect of SiO<sub>2</sub>-graphene oxide hybrid as inorganic nanofiller on corrosion protection properties of epoxy coatings," *Surface and Coatings Technology*, vol. 311, pp. 282–294, Feb. 2017, <https://doi.org/10.1016/j.surfcoat.2017.01.013>.
- [26] A. A. Khan, A. Khan, Z. Zafar, and I. Ahmad, "Insights into the corrosion mitigation efficacy of modified SiO<sub>2</sub>/GO-based epoxy composite coatings for aluminum alloy AA6061 in marine applications," *Journal of Coatings Technology and Research*, vol. 21, no. 4, pp. 1447–1466, July 2024, <https://doi.org/10.1007/s11998-023-00906-z>.
- [27] J. Gašiorek *et al.*, "Anticorrosion properties of silica-based sol-gel coatings on steel – The influence of hydrolysis and condensation conditions," *Ceramics International*, vol. 48, no. 24, pp. 37150–37163, Dec. 2022, <https://doi.org/10.1016/j.ceramint.2022.08.291>.
- [28] L. Liu, X. Guo, L. Shi, L. Chen, F. Zhang, and A. Li, "SiO<sub>2</sub> -GO nanofillers enhance the corrosion resistance of waterborne polyurethane acrylic coatings," *Advanced Composites Letters*, vol. 29, Jan. 2020, <https://doi.org/10.1177/2633366X20941524>.
- [29] N. Wang, H. Gao, J. Zhang, and P. Kang, "Effect of Graphene Oxide/ZSM-5 Hybrid on Corrosion Resistance of Waterborne Epoxy Coating," *Coatings*, vol. 8, no. 5, May 2018, Art. no. 179, <https://doi.org/10.3390/coatings8050179>.
- [30] A. Bouibed and R. Doufounne, "Synthesis and characterization of hybrid materials based on graphene oxide and silica nanoparticles and their effect on the corrosion protection properties of epoxy resin coatings," *Journal of Adhesion Science and Technology*, vol. 33, no. 8, pp. 834–860, Apr. 2019, <https://doi.org/10.1080/01694243.2019.1571660>.